

How to Cite:

Karkuzhali, S., & Puyalnithi, T. (2022). Deep learning based classification network for diagnosis of glaucoma in two dimensional retinal fundus images. *International Journal of Health Sciences*, 6(S4), 6957–6980. <https://doi.org/10.53730/ijhs.v6nS4.10285>

Deep learning based classification network for diagnosis of glaucoma in two dimensional retinal fundus images

Dr. S. Karkuzhali

Assistant Professor, Department of Computer Science and Engineering, Mepco Schlenk Engineering College, Sivakasi, Tamilnadu, India
Corresponding author email: karkuzhali@mepcoeng.ac.in

Dr. Thendral Puyalnithi

Assistant Professor (Sr. Grade), Department of Artificial Intelligence and Data Science, Mepco Schlenk Engineering College, Sivakasi, Tamilnadu, India
Email: thendralp@mepcoeng.ac.in

Abstract--Glaucoma is an eye condition which prompts lasting visual deficiency when the illness advances to a propelled stage. It happens because of high intraocular pressure inside the eye, bringing about harm to the optic nerve. Glaucoma doesn't show any side effects in its initial stage and in this manner, it is critical to analyze ahead of schedule to forestall visual impairment. Fundus photography is broadly utilized by ophthalmologists to aid analysis of glaucoma and is cost-effective. The utilization of Computer Aided Diagnosis(CAD) is successful in the conclusion of glaucoma and can help the clinicians to reduce their remaining task at hand altogether. We have likewise talked about the upsides of utilizing condition of-workmanship procedures, including Deep learning (DL), when building up the robotized framework. The DL techniques are powerful in glaucoma diagnosis. Novel DL calculations with large information accessibility are required to build up a dependable CAD framework. Such procedures can be utilized to analyze other eye diseases precisely. This paper examines the helpfulness of CAD frameworks and deep feed forward neural network to fairly analyze patients with glaucoma. Additionally, unique AI strategies utilized by scientists over the past decade are summarized. It is likewise been noticed that DL has points of interest over the customary machine learning procedures, whereby next to no hand-created highlights extraction and choice are required. Also, any social insurance professionals can exploit the CAD framework to help specialists in screening for glaucoma. This will be particularly useful in geological regions where ophthalmologists are scant. Besides, the CAD framework can likewise be actualized in the

location of glaucoma when other eye conditions should be screened for with Effective accuracy of 96% in classification.

Keywords---glaucoma, CAD, deep feed, neural network, dimensional retinal fundus images.

Introduction

Glaucoma is a degenerative eye disease, in which the optic nerve is damaged progressively that leads to loss of visual field and eventually to a state of irreversible blindness [1]. Figure 1 shows the effect of glaucoma in human vision. It is the second leading cause of blindness. The prevalent model estimates that approximately 11.1 million people will suffer from glaucoma worldwide in 2020 (Duo et al. 2012). Increased eye pressure called IOP plays a major role in damaging the delicate nerve fibers of the optic nerve. In some cases, glaucoma can develop in patients with normal range of IOP [2]. The patients with glaucoma have an IOP > 20mmHg, (normal people have IOP of ~ 10mmHg), which could damage patients' optic nerve in the posterior segment of the eyeball and cause blindness [3].



Figure 1 The effect of glaucoma in human vision. (a) Normal vision (b) Vision of patient with glaucoma

(Source: https://nei.nih.gov/health/glaucoma/glaucoma_facts)

The function of aqueous humor is to nourish the area around the iris and cornea, and it exerts pressure to maintain the shape of the eyeball. The fluid is produced continuously causing IOP. To maintain an IOP, this inflow is offset by drainage between the iris and cornea, primarily (80-90%) through a sponge like substance known as trabecular meshwork, and the remaining fluids drain independently. Clinicians use an ophthalmoscope to view inside the fundus image during an eye examination for detection of glaucoma.

Diagnostic test for glaucoma

Currently, three major diagnostic tests clinically practiced for detection of glaucoma are assessment of IOP, visual field testing and optic nerve head assessment.

- A. Assessment of IOP: The doctor uses a tonometer, a device used to measure IOP. This is not sensitive enough for early detection, and glaucoma can occur without increased eye pressure.
- B. Visual field testing: Visual field testing determines the area where the patient's vision is unusual. It identifies field of abnormal vision with specialized equipment which makes it unsuitable for a comprehensive screening of glaucoma except in sophisticated medical centers.
- C. Optic nerve head assessment: Optic nerve head assessment proves to be a very reliable method, but requires trained professionals, and it is a time-consuming, expensive and highly subjective method. Early occurrences of glaucoma are also detected using Optical Coherence Tomography (OCT) and Heidelberg Retinal Tomography (HRT) based on interferometric and confocal microscopic techniques.

Fundus images provide the magnified structural details of the microscopic OD, and these images have been used by clinicians as a cost-effective diagnostic tool. In the assessment of optic nerve, OD is the location where ganglion cell axons exit the eye to form optic nerve, through which visual information of the photoreceptors is transmitted to the brain. OD can be divided into central bright zone and peripheral zone called OC and neuroretinal rim [4]. Figure 2 shows the structural landmarks such as OD and OC of the retinal image.

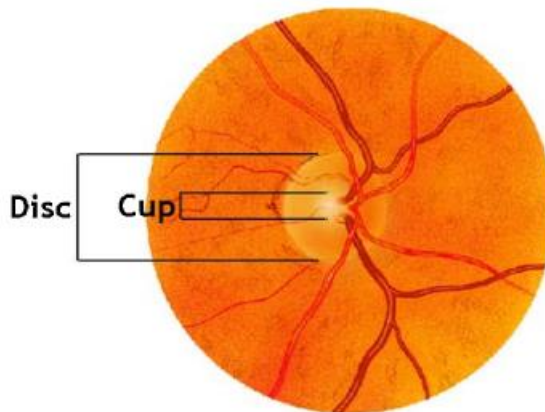


Figure 2 Retinal image with OD and OC.
(Source: Haleem, et al. 2013)

Structural indicators of glaucoma

The three main structural indicators of glaucoma are Cup-to-Disc Ratio (CDR), Inferior Superior Nasal Temporal (ISNT) ratio and Distance between OD center and Optic nerve head (DOO) [5]. They are explained below.

- A. Cup-to-Disc ratio: CDR measures change in the cup area by calculating the ratio between the areas of the OC to areas of the OD. The CDR value > 0.3 indicates that the risk of glaucoma is high. Due to the presence of glaucoma, the area of the cup will increase, resulting in shift of the optic nerve head towards the nasal side. This shift in position of center of the OD is computed

as a distance. Figure 3 shows a normal sized cup and a large cup damaged by glaucoma both in retinal image and diagrammatic illustration.

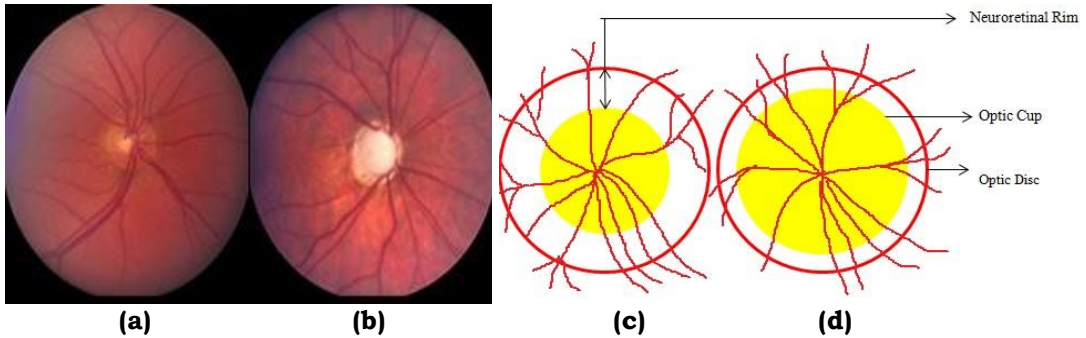
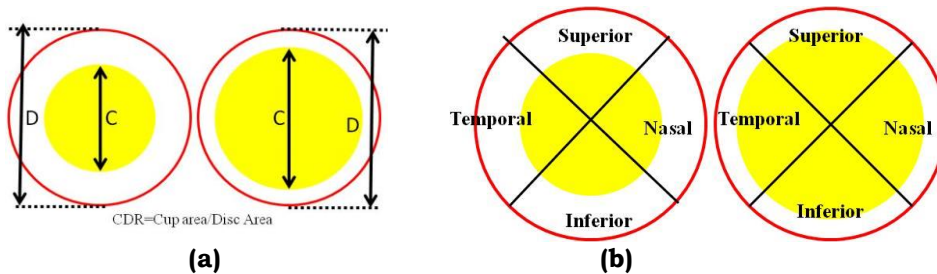


Figure 3 Retinal images (a) normal (b) glaucoma affected eye, and diagrammatic illustrations of (c) normal (d) glaucoma affected eye
 (Source <http://www.glaucoma.org/treatment/optic-nerve-cupping.php>)

- B. ISNT ratio: The neuroretinal rim decreases in size with concurrent enlargement of OC. The rim is usually the broadest in the inferior disc region, followed by the superior, then nasal and finally temporal called ISNT rule. Glaucoma damages the neuroretinal rim in inferotemporal and superotemporal regions, then followed by temporal and lastly in nasal region. The ratio of the sum of BVs area in inferior and superior regions to area of BVs in nasal and temporal regions is also the definition for ISNT rule. The indication of lower ISNT ratio increases the risk of presence of glaucoma.
- C. Distance between OD center and optic nerve head (DOO): The optic nerve head and center of OD are detected by identifying the area of the brightest intensity. The Euclidean distance between the center of OD is computed to detect the distance between OD center and Optic Nerve Head (ONH). The value is very high for normal eye. Figure 4 shows the diagrammatic representation of CDR, ISNT ratio and DOO.



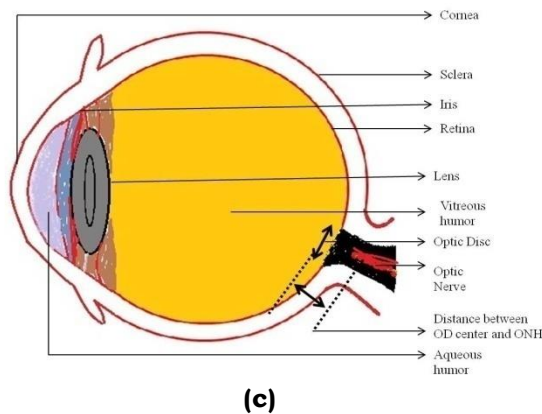


Figure 4 Diagrammatic illustration of structural indicators of glaucoma (a) Cup-to-Disc ratio (b) Inferior Superior Nasal Temporal ratio (c) Distance between center of OD and ONH

Several clinical indicators are considered as risk factors of glaucoma such as CDR, disc diameter, ISNT rule, PeriPapillary Atrophy (PPA) and notching. CDR and ISNT rule are commonly accepted by ophthalmologists for glaucoma evaluation.

Classification of glaucoma

Glaucoma can be broadly classified as Primary Open Angle Glaucoma (POAG) and Primary Closed Angle Glaucoma (PCAG).

- A. Primary open angle glaucoma: POAG is the most common form of glaucoma and is caused by slow-clogging condition of the drainage canals, resulting in increased eye pressure causing damage to optic nerve. POAG has wide and open angle between iris and cornea.
- B. Primary closed angle glaucoma: PCAG has a closed angle between iris and cornea. The iris is found to be blocking the drainage of aqueous humor through the trabecular meshwork. It is caused by blocked drainage canals, resulting in sudden rise in increased pressure. Figure 5 shows the types of glaucoma.

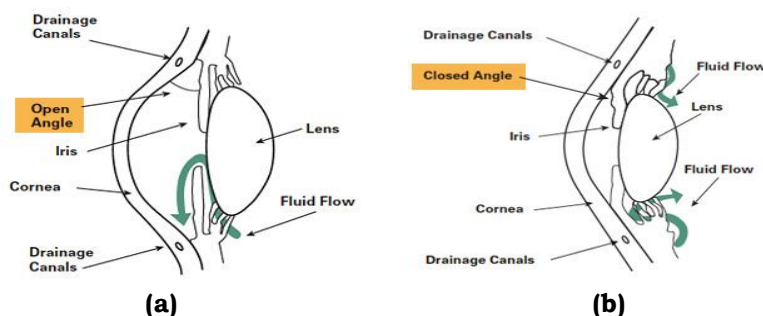


Figure 5 Classification of glaucoma (a) Primary open angle glaucoma (b) Primary closed angle glaucoma

(Source: <http://www.glaucoma.org/glaucoma/types-ofglaucoma.php>)

In this paper, we discuss about the role of computational intelligence algorithms in Glaucoma diagnosis in section 2. Methodology and Discussion in section 3 and 4. In section 5 and 6 discuss about the conclusion and summarization. The principle themes secured by this study might be listed as follows:

- ways to deal with segment different objects from both 2D and 3D retinal images;
- approaches that may prompt empowering results for glaucoma diagnosis;
- Challenges looked by specialists; and
- at present accessible retinal datasets and assessment techniques.

Literature Survey

Lee *et al.* (2019) assemble an AI based glaucoma analytic model using SAP information, author proposed few thoughts and approved them by means of a near investigation that incorporates numerical tests utilizing our gathered information. So as to reflect more data, new composite factors utilizing two visual field clustering techniques, the Garway-Heath map furthermore, glaucoma hemifield test (GHT) segment map, were utilized notwithstanding Total Deviation(TD)/Pattern Deviation(PD) esteems as info factors. The utilization of these new composite factors got from the TD/PD estimations of each group is a key commitment of this paper, which improves the expectation execution essentially. Four notable AI classifiers and four dimensionality decrease strategies were applied and looked at as far as arrangement exactness and AUC [6].

Jammal *et al.*(2019) contrasted the capacity of the Machine to Machine deep learning (M2M DL) calculation to that of human graders in recognizing eyes with glaucomatous visual field misfortune. We conjectured that the SD OCT-prepared M2M forecasts would have a more grounded connection with visual field measurements than abstract gradings by human specialists, accordingly giving an extra required approval of this methodology as a technique to screen for glaucomatous harm [7].

Baxter *et al.*(2019) To anticipate the requirement for careful intercession in patients with Primary open angle glaucoma (POAG) utilizing fundamental information in electronic health records (EHRs).Structured EHR information of 385 POAG patients from a solitary scholastic foundation were joined into models utilizing multivariable logistic regression,random forests, and artificial neural networks [8].

Yousefi. S *et al.* (2018) used Machine learning examination effectively recognizes patterns of Progression in glaucomatous eyes and surveys the progression along those patterns, in this way supporting our speculation that AI pattern examination is more touchy than worldwide investigation of MD, locale astute or point-wise investigation. We seen that AI was the most touchy way to deal with identify movement among (the best-performing), while worldwide MD examination was the least sensitivity [9].

Wang *et al.*(2020) bind together the structure investigation and capacity relapse to recognize glaucoma patients from ordinary controls successfully. In particular,

our technique works in two stages: a semi-supervised learning methodology with perfection supposition that is first applied for the substitute task of missing function regression labels. Thusly, the proposed perform multi-tasks learning system is fit for investigating the structure and function connection between the OCT images and visual field estimation all the while, which contributes to characterization execution improvement [10].

Claro *et al.*(2020) discusses that the feature extraction and classification are basic steps in the diagnosis of glaucoma. The author assessed the descriptors of texture, shape and CNNs. Our best outcome was accomplished by linking GLCM with CNNs, acquiring a fantastic Kappa record, and a precision of 93.35% for the improvement set and 92.78% for the performance set. We likewise checked that the proposed strategy functions admirably in any event, when there are blemishes in the OD segmentation [11].

Al-Akhras *et al.*(2019) dissected and includes were separated, at that point a classification for them was performed utilizing Support Vector Machines(SVM) and a Genetically-Optimized Artificial Neural Networks(ANN) AI techniques.For SVM classifier and when the arrangement depended on bothset of highlights without information standardization, the most noteworthy classifica-tion precision of 87.74% and the most elevated particularity of 100% wereobtained utilizing Gamma estimation of 0.25. The most noteworthy affectability valueof 23.08% was gotten utilizing the Gamma estimation of 1.When information standardization was utilized with both arrangement of fea-tures, the most elevated characterization exactness of 80.19% and the highestspecificity of 91.40% were acquired utilizing a Gamma estimation of 0.25.The most elevated affectability estimation of 30.77 was acquired utilizing a Gammavalue of 0.8.For ANN classifier got precision for the blend offeatures was 98% with and without information standardization [12].

Bisneto *et al.* (2020) follows the step to diagnose glaucoma, image acquisition through the RIM-ONE and Drishti-GS open databases ,training of a contingent Generative Adversarial Network for segmentation of the optic disc into retinal images; pre-processing through improvement and opening fill-in methods; extraction of texture properties utilizing the list of ordered decent variety; and approval of the proposition through three classifiers assessed by four performance measurements [13].

Ma *et al.*(2016) has designed and build up a shoe-coordinated sensing framework for objective bio-data assortment, use signal handling calculations for include estimation and influence AI just as factual investigation approaches for step design assessment. The created sensor stage is used in a randomized clinical preliminary led at UCLA Stein Eye Institute with 19 members. Our preliminary included both glaucoma patients and age-coordinated sound members per-shaping a progression of step tests. With the caught sensor information, we create signal preparing and AI calculations to give a quantitative examination between stride attributes in more established grown-ups with and without glaucoma [14].

Martins *et al.*(2020) diagnosing Glaucoma utilizing fundus pictures and run offline in cell phones. A few open datasets of fundus pictures were blended and used to construct Convolutional Neural Networks (CNNs) that perform division

what's more, order assignments. These systems are then used to assemble a pipeline for Glaucoma evaluation that yields a Glaucoma certainty level and furthermore gives a few morphological highlights and divisions of pertinent structures, bringing about an interpretable Glaucoma finding [15].

Orlanda *et al.* (2020) summed up the outcomes and discoveries from REFUGE, the main open test concentrated on glaucoma order and optic disc/cup segmentation from shading fundus images. We dissected the exhibition of every one of the twelve groups that took part in the on location version of the opposition, during MICCAI 2018. We saw that the best methodologies for glaucoma arrangement coordinated profound learning procedures with notable glaucoma explicit biomarkers, for example, changes in the vertical cup-to-circle proportion or retinal nerve fiber layer abandons. The two highest level groups, then again, accomplished preferred outcomes over two glaucoma experts, a promising sign towards utilizing mechanized strategies to distinguish glaucoma suspects with fundus imaging [16].

Kishore *et al.*(2020) At first, the fundus pictures are exposed to preprocessing followed by highlight extraction and highlight combination by Intra-Class and Extra-Class Discriminative Correlation Analysis (IEDCA). The element combination approach disposes of between-class connection while holding adequate Feature Dimension (FD) for Correlation Analysis (CA). The intertwined highlights are then taken care of to the classifiers to be specific Support Vector Machine (SVM), Random Forest (RF) and K-Nearest Neighbor (KNN) for characterization separately. At last, Classifier combination is likewise structured which joins the choice of the gathering of classifiers dependent on Consensus-based Combining Method (CCM) [17].

Phene *et al.* (2019) developed an deep learning algorithm calculation with higher affectability and practically identical particularity to eye care suppliers in recognizing referable glaucomatous optic neuropathy (GON) in shading fundus pictures. The calculation's forecast of referable GON looked after great execution on a free dataset with analyze in view of a full glaucoma workup. Moreover, our work gives understanding into which Optic nerve head(ONH) highlights drive GON evaluation by glaucoma experts. These experiences may help to improve clinical choices for alluding patients to glaucoma experts dependent on ONH discoveries during diabetic fundus picture appraisals [18].

Hu *et al.*(2020) depict the methodologies and perimetric tests used to assess glaucomatous visual field movement and variables that are significant for distinguishing movement. These incorporate boost size, which region of the visual field to evaluate (focal versus fringe), and the testing recurrence, which is essential to distinguish change early while limiting patient testing trouble. We additionally survey the distinctive factual techniques created to distinguish change. These incorporate pattern and occasion based examinations, parametric and non-parametric tests, populace based versus individualized methodologies, just as pointwise what's more, worldwide examinations. [19].

Gour *et al.*(2019) expected to build up a mechanized symptomatic framework dependent on fundus pictures for glaucoma illness. It centers around extraction of GIST and pyramid histogram of oriented gradients (PHOG) highlights from

preprocessed fundus pictures. The separated highlights are positioned and chosen through principal component analysis (PCA) to pick noteworthy highlights. The order into glaucomatous pictures is finished with SVM classifier on fundus pictures of Drishti-GS1 and HRF databases [20]. Maheshwari *et al.* (2019) presented bit-plane slicing (BPS) and local binary patterns (LBP) based novel methodology for glaucoma analysis. Right off the bat, methodology isolates the red (R), green (G), and blue (B) channels from the info shading fundus picture and parts the channels into bit planes. Furthermore, extricate LBP based factual highlights from every one of the bit planes of the individual channels. Thirdly, these highlights from the individual channels are taken care of independently to three different support vector machines (SVMs) for classification. At long last, the choices from the individual SVMs are melded at the choice level to arrange the information fundus picture into typical or glaucoma class [21].

Chan *et al.* (2019) have utilized optical coherence tomography angiogram (OCTA) pictures for robotized glaucoma location. Visual field (VF) from the left eye while ocular dexter (OD) were acquired from right eye of subjects. We have utilized OS macular, OS disc, OD macular and OD plate pictures. In this work, nlocal phase quantization (LPQ) method was applied to separate the highlights. Data combination and PCA are utilized to join and lessen the highlights [22]. Raghavendra *et al.* (2018) proposed a novel CAD device for the precise discovery of glaucoma utilizing profound learning procedure. An eighteen layer convolutional neural systems (CNN) is viably prepared so as to remove powerful highlights from the computerized fundus pictures. At last these highlights are characterized into typical and glaucoma classes during testing. We have accomplished the most elevated exactness of 98.13% utilizing 1426 (589: typical and 837: glaucoma) fundus pictures. Our test results exhibits the heartiness of the framework, which can be utilized as a strengthening instrument for the clinicians to approve their choices [23]. Asaoka *et al.* (2016) used to identify Preperimetric glaucoma VFs were characterized as all VFs before a first finding of show glaucoma (Anderson-Patella's measures). Altogether, 171 PPGVFs from 53 eyes in 51 OAG patients and 108 VFs from 108 sound eyes in 87 sound members were broke down (all VFs were tried utilizing the Humphrey Field Analyzer 30-2 program; Carl Zeiss Meditec, Dublin, CA). The 52 complete deviation, mean deviation, and example standard deviation values were utilized as indicators in the DL classifier: a profound feed-forward neural network (FNN), alongside other ML strategies, including random forest (RF), SVM and NN [25].

Mohamed *et al.* (2019) performed preprocessing strategies to cater for noise removal and illumination correction. This is underscored in the usage of the anisotropic dispersion channel and illumination correction method. The pixels of the input image are then aggregate into superpixels utilizing Simple Linear Iterative Clustering (SLIC) approach. At that point, picture features based on histogram information and textural data are extricated on each superpixel with statistical pixel-level (SPL) strategy. The noticeable highlights are then taken care of into Support Vector Machine (SVM) classifier to classify each superpixel into OD, OC, vein, and foundation areas. The classifier is also used to decide the limits of both OD and OC. Ultimately, the divided optic disc and optic cup are utilized to decide the nearness of glaucoma utilizing CDR estimation [26].

Mvoulana *et al.*(2019) propose another completely computerized system for glaucoma screening and determination from retinal fundus pictures. So as to permit eye assessment in remote areas with restricted access to clinical offices, center in this work around the improvement of a computationally-productive calculation for additional usage on cell phones. To begin with, the technique gives a vigorous OD location strategy, consolidating a splendor model and a layout coordinating procedure, to adequately identify the OD even within the sight of splendid injuries related to obsessive cases. Second, a proficient OC and OD division is performed, utilizing a surface based and model-based methodology. At long last, Cup-to-Disk Ratio (CDR) calculation prompts glaucoma screening with a characterization among solid and glaucomatous patients. The technique accomplishes 98% of accuracy in DRISHTI-GS1 dataset on definite glaucoma screening and finding, and incredible execution rates on assessment measurements, beating the best in class CDR highlight based approaches. [27].

dos Santos Ferreira *et al.*(2018) presented the improvement of a strategy for the programmed location of glaucoma in retinal pictures utilizing a profound learning approach along with the investigation of surface properties through phylogenetic assorted variety files. The approach utilized is as per the following: First, picture securing is done from the RIM-ONE, DRIONSDB, furthermore, DRISHTI-GS databases, trailed via preparing the convolutional neural arrange for OD segmentation. After this division, it is important to perform evacuation of the veins after which include extraction is applied to the pictures produced from the RGB channels and the dark levels. The separated qualities depend just on the highlights of surface utilizing phylogenetic decent variety files. Characterization was performed utilizing a methodology dependent on the convolutional neural system. The performance measures like accuracy, sensitivity, and specificity in 100% [28].

Raghavendra *et al.*(2018) proposed a novel region based optic plate division followed by the Radon transformation (RT). The adjustment in the brightening levels of Radon changed picture are repaid utilizing modified census transformation (MCT). The MCT pictures are at that point exposed to GIST descriptor to separate the spatial envelope vitality range. The acquired measurement of the GIST descriptor is diminished utilizing locality sensitive discriminant analysis(LSDA) trailed by different component determination and positioning plans. The positioned highlights are used to manufacture a proficient classifier to distinguish glaucoma. The framework yielded a most extreme accuracy (97.00%), sensitivity (97.80%) and specificity (95.80%) [29].

Maheshwari, *et al.*(2017) used Variational mode decomposition (VMD) technique is utilized in an iterative way for picture decay. Different highlights to be specific, Kapoor entropy, Renyi entropy, Yager entropy, and fractal measurements are extricated from VMD segments. ReliefF calculation is utilized to choose the prejudicial highlights and these highlights are then taken care of to the least squares SVM (LS-SVM) for classification. Our proposed strategy accomplished classification accuracy of 95:19% and 94:79% utilizing three-overlap and ten times cross-approval techniques, separately SVM classifier with nineteen highlights. [30]

Kausu *et al.*(2018) proposed a novel strategy for glaucoma recognizable proof dependent on time-invariant element CDR proportion what's more, anisotropic dual-tree complex wavelet transform features. OD segmentation is done by utilizing Fuzzy C-Means grouping technique and Otsu's thresholding is utilized for optic cup division. The outcomes show the proposed strategy accomplished an exactness pace of 97.67% with 98% sensitivity utilizing a multilayer perceptron model that is considered as clinically noteworthy when contrasted with the current works [31].

Bowd *et al.*(2020) compared gradient boosting classifiers prepared on blends of entire picture and provincial OCTA and OCT macula and optic nerve head boundaries to individual OCTA and OCT boundaries for grouping pictures from solid and glaucoma eyes. In the best case, the full GBC (that joined all chose OCTA and OCT boundaries) indicated preferable analytic precision over everything except 3 individual boundaries. Gradient boosting classifiers performed well at the order task with AUROCs going from 0.90 to 0.93. These outcomes appear guarantee for joining auxiliary estimations (for example vessel thickness and tissue thickness) acquired from two Avanti examining conventions (for example macula and ONH) for improved location of ahead of schedule to direct glaucoma [32]. The past surveys distributed in this area were clinical or centered on conventional AI calculations or accentuated a specific illness or on the other hand concentrated on equipment execution of artificial intelligence in ophthalmic conclusion[33][34][35][36][37][38][39][40][41].

Thakur *et al.*(2018) introduced about different division and classification approaches utilized till date for glaucoma conclusion. It summarises various challenges in the field of division and classification which can be thought about to take care of an issue using improved picture preparing approaches. Studies show that there are still a few highlights which can be mulled over for improving the presentation of arrangement. There stays a challenge to keep away from under division or over-division of discs and cup with enormous or little sizes because of direction of retinal vessels and peripapillary decay which crumbles the exhibition of segmentation. To conquer the talked about issues, segmentation of optic circle is normally accomplished in the red channel as this channel has the most noteworthy uniqueness between non-plate and circle region. The area of intrigue is typically distinguished before preparing as it reduces the size of the information picture and makes the calculations faster and precise. Difficulties in the division of optic disc are because of the nearness of vessels which are overwhelmed by the preparing picture that uses morphological activities like opening, shutting or histogram leveling. Additionally, division of optic cup is viewed as progressively repetitive when contrasted with optic plate due to the interweavement of optic cup with veins and surrounding tissues. Its division is normally conveyed in the green channel of RGB shading space because of less perceivability of retinal vessels in this channel. Be that as it may, from the current methodologies of segmentation, the presentation of grouping based division is better than others. Additionally, SVM classifier is the regularly utilized classifier with greatest exactness. Thus, improved division and classification approach should be proposed to analyze the disease glaucoma [42].

Zilly *et al.*(2017) proposed CNN propelled group learning engineering has been appeared to better the best in class on the open DRISHTI-GS informational index. From an examination perspective our work makes two principle commitments. Initial, a novel entropy testing technique is suggested that permits the calculation to impressively diminish its computational exertion while performing better than the straightforward uniform examining approach. Besides, building upon this procedure, a unique system for learning convolutional channels in a principled way utilizing reweighted boosting was depicted. The point behind this learning structure is twofold. Initial, a novel method of preparing convolutional channels in a system design was investigated. Second, we expect the proposed technique will be progressively amiable to hypothetical bits of knowledge into the central standards administering CNNs or even profound neural systems (DNN) all in all. These experiences may be founded on the acknowledgment that a considerable lot of the attributes of the proposed strategy are proportional to gathering learning frameworks [43].

Divya *et al.*(2018) discussed about two techniques for highlight choice: the Student's t-test and PCA for the screening of glaucoma utilizing fundus pictures. The altered dynamic methodology on classifier yield dependent on a mix of R, G, B and Gray segments accomplished a decent arrangement precision contrasted with autonomous yield from various channels. Utilizing 2D EWT the sub-band pictures were isolated and correntropy was utilized for highlight extraction. Understudy's t-test and z-score standardization was utilized for highlight determination and positioning. In the second technique for include choice PCA was utilized. Here PCA was utilized to lessen the dimensionality. At that point Least Square Support Vector Machine (LS-SVM) is utilized as classifier with RBF as the bit. The execution of the classifier yield utilizing bit-wise OR activity was assessed. It is seen that the bit-wise OR activity has exactness around 99 % for RGBGrey channel consolidated together [44].

de Carvalho Junior *et al.*(2018) introduced a programmed strategy through which picture handling and example acknowledgment procedures can effectively satisfy the assignment of giving a second sentiment to the authority in regards to adjustments in the optic nerve that cause glaucoma. To begin with, the strategy utilizes the Otsu and k-implies calculations in the division errand of the optic circle area. At that point, the surface qualities are extricated utilizing the phylogenetic decent variety records. At long last, we utilized different classifiers to check the power of the strategy. An examination of the consequences of the correlation of the Otsu and k-implies calculations shows that the two strategies present promising results. The Otsu calculation yields especially encouraging outcomes. With respect to channels, the red divert was increasingly proficient in the measurement assignment of glaucoma. The files of phylogenetic assorted variety proposed in this examination were effective for the errand of portraying the optic circle locales. It was conceivable to accomplish promising outcomes utilizing the two strategies: we accomplished qualities above 99% in all measurements for assessing the outcomes. At long last, it is accepted that the proposed strategies can be incorporated into a PC helped conclusion instrument to be applied in genuine situations and can give a second conclusion to a specialist. This is a quicker and less tiring methods for the master to accomplish an all the more patient friendly determination for glaucoma [45].

Singh et al. (2016) presented a programmed picture handling based strategy for glaucoma determination from the advanced fundus picture. In this paper wavelet highlight extraction has been trailed by improved hereditary element choice joined with a few learning algorithms and different boundary settings. Dissimilar to the current examination works where the features are considered from the total fundus or a sub picture of the fundus, this work is dependent on highlight extraction from the fragmented and vein evacuated optic circle to improve the precision of recognizable proof. The test results introduced in this paper indicate that the wavelet highlights of the divided optic circle picture are clinically more significant in contrast with highlights of the entire or sub fundus picture in the discovery of glaucoma from fundus picture. Precision of glaucoma recognizable proof accomplished in this work is 94.7% and an examination with existing strategies for glaucoma identification from fundus image indicates that the proposed approach has improved exactness of characterization [46].

Boquete et al. (2014) discussed about multifocal electroretinogram (mfERG) is an as of late created indicative strategy that gives objective spatial information on the visual pathway and might be of possible advantage in early conclusion of glaucoma. This paper investigations 13 morphological attributes that characterize mfERG accounts and groups them utilizing a spiral premise work arrange prepared with the Extreme Learning Machine calculation. At the point when used to distinguish glaucomatous parts, the technique proposed produces affectability furthermore, particularity estimations of over 0.8 [47].

Acharya et al. (2017) developed an effective framework structured by misusing a few calculations from imaging innovation. The shading pictures are changed over to its dim scale utilizing versatile histogram evening out. The dim scale pictures are at that point convolved with four sorts of channel banks specifically; Leung-Malik, Schmid, MR4 and MR8 to acquire textons. Textons speak to essential components in characteristic pictures. Higher request spectra help in the extraction of otherworldly highlights from textons and successive coasting forward hunt technique joined with t-test is utilized to choose the unmistakable highlights what's more, kill the excess highlights. It is discovered that kNN classifier for LM channel bank delivered the most elevated exactness of 95.8%, explicitness of 92.3%, the affectability of 96.7% furthermore, PPV of 98% utilizing just six noteworthy features [48].

Mitra et al. (2018) discussed about ROI recognition as a lone relapse bind, from picture pixel esteems to return for money invested facilitates including class probabilities. A Convolution Neural Network (CNN) has prepared on full pictures to foresee jumping boxes alongside their comparable to probabilities and certainty scores. The publically accessible MESSIDOR and Kaggle datasets have been utilized to prepare the system. We embraced different information expansion strategies to intensify our dataset with the goal that our system turns out to be less delicate to commotion. From a very significant level viewpoint, each picture is separated into a 13 X 13 network. Each lattice cell conceives 5 jumping boxes alongside the relating class likelihood and a certainty score. Prior to preparing, the system and the bouncing box priors or grapples are introduced utilizing k-implies grouping on the first dataset utilizing a separation metric dependent on

Intersection of the Union (IOU) over ground-truth jumping boxes. During preparing indeed, a aggregate squared misfortune work is utilized as the prediction"s blunder work. At last, Non-most extreme concealment is applied by the proposed philosophy to arrive at the closing expectation [49].

Issac et al.(2015) discussed ROI recognition as a lone relapse bind, from picture pixel esteems to return for money invested facilitates including class probabilities. A Convolution Neural Network (CNN) has prepared on full pictures to foresee jumping boxes alongside their comparable to probabilities and certainty scores. The publically accessible MESSIDOR and Kaggle datasets have been utilized to prepare the system. We embraced different information expansion strategies to intensify our dataset with the goal that our system turns out to be less delicate to commotion. From a very significant level viewpoint, each picture is separated into a 13 X 13 network. Each lattice cell conceives 5 jumping boxes alongside the relating class likelihood and a certainty score. Prior to preparing, the system and the bouncing box priors or grapples are introduced utilizing k-implies grouping on the first dataset utilizing a separation metric dependent on Intersection of the Union (IOU) over ground-truth jumping boxes. During preparing indeed, a aggregate squared misfortune work is utilized as the prediction"s blunder work. At last, Non-most extreme concealment is applied by the proposed philosophy to arrive at the closing expectation [50].

Miri et al.(2017) Bruch's membrane opening-minimum rim width (BMO-MRW) is an as of late proposed basic boundary which assesses the remaining nerve fiber packs in the retina and is better than other traditional auxiliary boundaries for diagnosing glaucoma. Estimating this basic boundary requires distinguishing proof of BMO areas inside phantom space optical cognizance tomography (SD-OCT) volumes. While most mechanized methodologies for division of the BMO either portion the 2D projection of BMO focuses or distinguish BMO focuses in singular B-checks, in this work, we propose an AI chart based methodology for genuine 3D division of BMO from glaucomatous SD-OCT volumes. The issue is planned as an advancement issue for finding a 3D way inside the SD-OCT volume. Specifically, the SD-OCT volumes are moved to the spiral space where the shut circle BMO focuses in the first volume structure a way inside the outspread volume. The assessed area of BMO focuses in 3D are recognized by finding the anticipated area of BMO focuses utilizing a diagram hypothetical methodology and planning the anticipated areas onto the Bruch's film (BM) surface. Dynamic writing computer programs is utilized so as to discover the 3D BMO areas as the base expense way inside the volume. So as to process the cost work required for finding the base cost way, an arbitrary timberland classifier is used to become familiar with a BMO model, got by extricating force highlights from the volumes in the preparation set, and registering the necessary 3D cost work. The proposed technique is tried on 44 glaucoma patients and assessed utilizing manual outlines. Results show that the proposed technique effectively recognizes the 3D BMO areas and has fundamentally littler mistakes analyzed to the current 3D BMO recognizable proof methodologies [51].

Medeiros et al.(2019) created and approved a novel DL calculation to evaluate optic plate photos for the nearness of glaucomatous harm. Rather than past works in this zone, our calculation was fit for yielding constant forecasts of

evaluated RNFL thickness, in this manner taking into account quantitative appraisal of the measure of neural harm on circle photos. This was accomplished via preparing the system with RNFL thickness estimations removed from SD OCT [52].

Meriaudeau et al.(2018) discussion will address the most recent Computer Aided Diagnosis procedures applied to phantom spectral domain optical coherence tomography (SD-OCT) just as Fundus Images. It will cover the premise of preprocessing to AI with approaches in view of Bag of Features, Bag of Word, Feature decrease, just as the most recent Deep Learning structures either utilized for division (vessels) or grouping [53].

Mookiah et al.(2012) surveyed utilizing optical coherence tomography, scanning laser polarimetry (SLP), and Heidelberg Retina Tomography (HRT) filtering techniques. These strategies are costly and consequently a novel ease robotized glaucoma finding framework utilizing advanced fundus pictures is proposed. The author examines the framework for the mechanized recognizable proof of typical and glaucoma classes utilizing Higher Order Spectra (HOS) and Discrete Wavelet Transform (DWT) highlights. The removed highlights are taken care of to the Support Vector Machine (SVM) classifier with direct, polynomial request 1, 2, 3 and Radial Basis Function (RBF) to choose the best bit work for mechanized dynamic. In this work, SVM classifier with part capacity of polynomial request 2 had the option to distinguish the glaucoma and ordinary pictures consequently with an exactness of 95%, affectability and explicitness of 93.33% and 96.67% separately. At long last, we have proposed a novel coordinated file called Glaucoma Risk Index (GRI) which is comprised of HOS and DWT highlights, to analyze the obscure class utilizing a solitary component. We trust that this GRI will help clinicians to make a quicker glaucoma analysis during the mass screening of ordinary/glaucoma pictures [54].

Niwas et al.(2016) addressed Anterior Segment Optical Coherence Tomography(AS-OCT) image quality assessment issue, we define a method for objective assessment of AS-OCT images using complex wavelet based local binary pattern features. These features are pooled using the Naïve Bayes classifier to obtain the final quality parameter. To evaluate the proposed method, a subjective assessment has been performed by clinical AS-OCT experts, who graded the quality of AS-OCT images on a scale of good, fair, and poor. This was done based on the ability to identify the AC structures including the position of the scleral spur [55].

Niwas et al.(2016) developed completely robotized strategy for ordering diverse ACG mechanismsbased on AS-OCT pictures is proposed. Since the manual analysis basically dependent on themorphology of every system, in this examination, a total arrangement of morphological highlights isextracted legitimately from crude AS-OCT pictures utilizing compound picture changes, from whicha little arrangement of useful highlights with least excess are chosen and taken care of into a Naïve Bayes Classifier (NBC) [56].

Asaoka et al.(2017) approve the value of the 'Arbitrary Forests' classifier to analyze early glaucoma with ghashtly SD-OCT [57].Cheng et al.(2012) A ensemble

kernel classifier is by coordinating a integrating kernel PCA(KPCA)with a help SVM as well as a immune clonal selection algorithm (ICSA).The KPCA approach is utilized to extricate features,where as the SVM procedure is utilized to bargain with classification,and the ICSA is applied to improve the boundaries of the proposed scheme.The proposed gathering classifier can consequently choose the portion type and advance its boundary sets, so as to create different SVM classifiers with various kernels. Regard less of whether the data is direct or non linear,an ideal characterization result can be acquired [58].

Acharya et al. (2015) proposed a novel computerized glaucoma conclusion strategy utilizing different highlights separated from Gabor change applied on advanced fundus pictures. In this work, we have utilized 510 pictures to group into ordinary and glaucoma classes. Different highlights namely mean, fluctuation, skewness, kurtosis, vitality, and Shannon, Rényi, and Kapoor entropies are extracted from the Gabor change coefficients. These separated highlights are exposed to head segment examination (PCA) to lessen the dimensionality of the highlights. At that point these highlights are positioned utilizing different positioning strategies to be specific: Bhattacharyya space calculation, t-test, Wilcoxon test, Receiver Operating Curve(ROC), and entropy. In this work, t-test positioning technique yielded the best with a normal exactness of 93.10%, affectability of 89.75% and explicitness of 96.20% utilizing 23 highlights with Support Vector Machine (SVM) classifier. Likewise, we have proposed a Glaucoma Risk Index (GRI) created utilizing principal components to group the two classes utilizing only one number [59].

Rehman et al.(2018) presented a multi-parametric optic plate discovery and limitation technique for retinal fundus pictures utilizing district based factual and textural highlights. Profoundly discriminative highlights are chosen based on the common data rule and a similar investigation of four benchmark classifiers: Support Vector Machine, Random Forest(RF), AdaBoost and RusBoost is introduced. The consequences of the proposed RF classifier based pipeline show its exceptionally serious execution (exactnesses of 0.993, 0.988 and 0.993 on the DRIONS, MESSIDOR and ONHSD databases) with the cutting edge, in this manner making it an appropriate contender for tolerant administration frameworks for early analysis of the Glaucoma [60].

Methodology

Deep learning algorithm deep feed forward neural network is used for training the model. The input fundus image will be 1700x1700 is used for training the Deep feed forward neural network. The proposed model has deep feed forward neural network with necessary number of convolution and filters layers, so the image in the final convolution layer will be ready enough to train the Fully Connected Feedforward network. The label for each image is normal or glaucoma affected image. The glaucoma affected images will be decided by an expert, ophthalmologist, by analyzing the presence of cup to disc ratio, ISNT ratio and distance between OD center and Optic nerve head. The infrastructure of the deep feed forward convolution neural network for number of convolution, pooling layers and ordering of convolution and pooling layers is set based on the input images. The training and testing and its validation and verification is performed. The

figure 3 shows the deep feed forward neural network based model to diagnose the presence of Glaucoma in the retinal image.

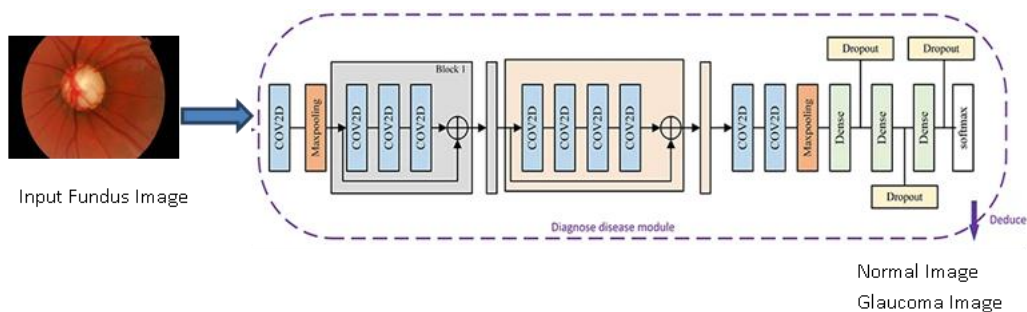


Fig 6: Proposed methodology for diagnosis of Glaucoma in Retinal fundus images.

Discussion

There are several publicly available databases for research purpose which have been provided by research organizations and educational institutes all over the world are MESSIDOR, DRIONS and ONHSD have been used for testing and evaluating the developed algorithms. The comparison of performance of deep learning algorithm in various dataset is tabulated below. The performance measures like Sensitivity(SE), Specificity(SPE), and Accuracy(Acc) are evaluated and compared in the below table and graph.

Table 1: Comparison of performance of proposed method and Existing Method

Database	Methods	SE	SPE	Acc
MESSIDOR	Xception	0.89	0.94	92
	Inception V3	0.91	0.96	94
	ResNet50	0.86	0.99	93
	DenseNet121	0.84	0.97	92
	VGG16	0.79	0.99	91
DRIONS	COG NET	0.95	0.99	95
	Xception	0.87	0.93	91
	Inception V3	0.89	0.92	92
	ResNet50	0.91	0.93	91
	DenseNet121	0.93	0.97	89
ONHSD	VGG16	0.79	0.92	86
	COG NET	0.95	0.99	96
	Xception	0.87	0.92	91
	Inception V3	0.86	0.91	93
	ResNet50	0.91	0.9	92

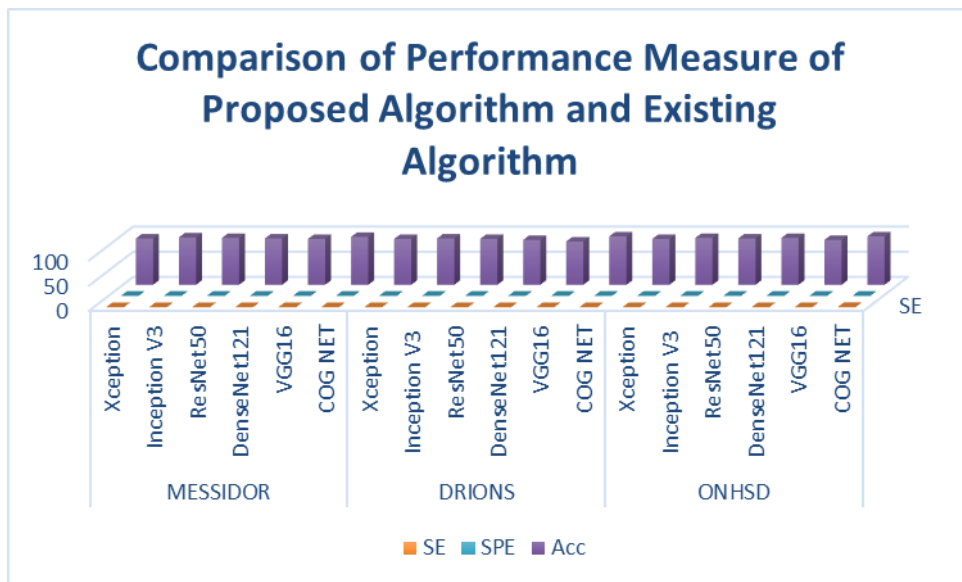


Fig 7: Graphical Representation of Comparison of performance of proposed method and Existing Method

Conclusion

This paper examines the helpfulness of CAD frameworks to fairly analyze patients with glaucoma. Additionally, unique AI strategies utilized by scientists over the past decade are summarized. It is likewise been noticed that DL has points of interest over the customary machine learning procedures, whereby next to no hand-created highlights extraction and choice are required. Also, any social insurance professionals can exploit the CAD framework to help specialists in screening for glaucoma. This will be particularly useful in geological regions where ophthalmologists are scant. Besides, the CAD framework can likewise be actualized in the location of glaucoma when other eye conditions should be screened for.

References

1. Lim, T. C., Chattopadhyay, S., & Acharya, U. R. A survey and comparative study on the instruments for glaucoma detection. *Medical engineering & physics*, 34(2), 129-139. (2012).
2. Dua, S., Acharya, U. R., Chowriappa, P., & Sree, S. V. Wavelet-based energy features for glaucomatous image classification. *Ieee transactions on information technology in biomedicine*, 16(1), 80-87. (2011).
3. Lin, J. C. H., Zhao, Y., Chen, P. J., Humayun, M., & Tai, Y. C. Feeling the pressure: A parylene-based intraocular pressure sensor. *IEEE Nanotechnology Magazine*, 6(3), 8-16. (2012).
4. Cheng, J., Liu, J., Xu, Y., Yin, F., Wong, D.W.K., Tan, N.M., Tao, D., Cheng, C.Y., Aung, T. and Wong, T.Y.. Superpixel classification based optic disc and optic cup segmentation for glaucoma screening. *IEEE transactions on medical imaging*, 32(6), 1019-1032. (2013)

5. Nayak, J., Acharya, R., Bhat, P. S., Shetty, N., & Lim, T. C. Automated diagnosis of glaucoma using digital fundus images. *Journal of medical systems*, 33(5), 337. (2009).
6. Lee, S. D., Lee, J. H., Choi, Y. G., You, H. C., Kang, J. H., & Jun, C. H. Machine learning models based on the dimensionality reduction of standard automated perimetry data for glaucoma diagnosis. *Artificial intelligence in medicine*, 94, 110-116. (2019).
7. Jammal, A.A., Thompson, A.C., Mariottoni, E.B., Berchuck, S.I., Urata, C.N., Estrela, T., Wakil, S.M., Costa, V.P. and Medeiros, F.A., Human versus machine: comparing a deep learning algorithm to human gradings for detecting glaucoma on fundus photographs. *American Journal of Ophthalmology*, 211, pp.123-131. (2020)
8. Baxter, S. L., Marks, C., Kuo, T. T., Ohno-Machado, L., & Weinreb, R. N. Machine learning-based predictive modeling of surgical intervention in glaucoma using systemic data from electronic health records. *American Journal of Ophthalmology*, 208, 30-40. (2019).
9. Yousefi, S., Kiwaki, T., Zheng, Y., Sugiura, H., Asaoka, R., Murata, H., Lemij, H. and Yamanishi, K.,. Detection of longitudinal visual field progression in glaucoma using machine learning. *American journal of ophthalmology*, 193, pp.71-79.(2018)
10. Wang, X., Chen, H., Ran, A.R., Luo, L., Chan, P.P., Tham, C.C., Chang, R.T., Mannil, S.S., Cheung, C.Y. and Heng, P.A.,. Towards multi-center glaucoma OCT image screening with semi-supervised joint structure and function multi-task learning. *Medical Image Analysis*, 63, 101695. (2020)
11. Claro, M., Veras, R., Santana, A., Araújo, F., Silva, R., Almeida, J., & Leite, D. An hybrid feature space from texture information and transfer learning for glaucoma classification. *Journal of Visual Communication and Image Representation*, 64, 102597. (2019).
12. Al-Akhras, M., Alawairdhi, M., & Habib, M.. Using soft computing techniques to diagnose Glaucoma disease. *Journal of Infection and Public Health*. PP.8 (2019)
13. Bisneto, T. R. V., de Carvalho Filho, A. O., & Magalhães, D. M. V. Generative adversarial network and texture features applied to automatic glaucoma detection. *Applied Soft Computing*, 90, 106165. (2020).
14. Ma, Y., Amini, N., & Ghasemzadeh, H. (2016). Wearable sensors for gait pattern examination in glaucoma patients. *Microprocessors and Microsystems*, 46, 67-74.
15. Martins, J., Cardoso, J. S., & Soares, F. (2020). Offline computer-aided diagnosis for Glaucoma detection using fundus images targeted at mobile devices. *Computer Methods and Programs in Biomedicine*, 192, 105341.
16. Orlando, J.I., Fu, H., Breda, J.B., van Keer, K., Bathula, D.R., Diaz-Pinto, A., Fang, R., Heng, P.A., Kim, J., Lee, J. and Lee, J., 2020. Refuge challenge: A unified framework for evaluating automated methods for glaucoma assessment from fundus photographs. *Medical image analysis*, 59, p.101570.
17. Kishore, B., & Ananthamoorthy, N. P. (2020). Glaucoma classification based on intra-class and extra-class discriminative correlation and consensus ensemble classifier. *Genomics*.
18. Phene, S., Dunn, R.C., Hammel, N., Liu, Y., Krause, J., Kitade, N., Schaekermann, M., Sayres, R., Wu, D.J., Bora, A. and Semturs, C., Deep learning and glaucoma specialists: the relative importance of optic disc

- features to predict glaucoma referral in fundus photographs. *Ophthalmology*, 126(12), pp.1627-1639.(2019)
19. Hu, R., Racette, L., Chen, K. S., & Johnson, C. A. FUNCTIONAL ASSESSMENT OF GLAUCOMA PROGRESSION: UNCOVERING PROGRESSION. *Survey of Ophthalmology*, (2020).
 20. Gour, N., & Khanna, P. Automated glaucoma detection using GIST and pyramid histogram of oriented gradients (PHOG) descriptors. *Pattern Recognition Letters*. (2019).
 21. Maheshwari, S., Kanhangad, V., Pachori, R. B., Bhandary, S. V., & Acharya, U. R. Automated glaucoma diagnosis using bit-plane slicing and local binary pattern techniques. *Computers in Biology and Medicine*, 105, 72-80. (2019).
 22. Chan, Y. M., Ng, E. Y. K., Jahmunah, V., Koh, J. E. W., Lih, O. S., Leon, L. Y. W., & Acharya, U. R. (2019). Automated detection of glaucoma using optical coherence tomography angiogram images. *Computers in biology and medicine*, 115, 103483.
 23. Raghavendra, U., Fujita, H., Bhandary, S. V., Gudigar, A., Tan, J. H., & Acharya, U. R. Deep convolution neural network for accurate diagnosis of glaucoma using digital fundus images. *Information Sciences*, 441, 41-49. (2018).
 24. Sarhan, A., Rokne, J., & Alhaji, R. (2019). Glaucoma detection using image processing techniques: A literature review. *Computerized Medical Imaging and Graphics*, 78, 101657. (2019).
 25. Asaoka, R., Murata, H., Iwase, A., & Araie, M. (2016). Detecting preperimetric glaucoma with standard automated perimetry using a deep learning classifier. *Ophthalmology*, 123(9), 1974-1980.
 26. Mohamed, N. A., Zulkifley, M. A., Zaki, W. M. D. W., & Hussain, A. An automated glaucoma screening system using cup-to-disc ratio via Simple Linear Iterative Clustering superpixel approach. *Biomedical Signal Processing and Control*, 53, 101454. (2019).
 27. Mvoulana, A., Kachouri, R., & Akil, M. (2019). Fully automated method for glaucoma screening using robust optic nerve head detection and unsupervised segmentation based cup-to-disc ratio computation in retinal fundus images. *Computerized Medical Imaging and Graphics*, 77, 101643.
 28. dos Santos Ferreira, M. V., de Carvalho Filho, A. O., de Sousa, A. D., Silva, A. C., & Gattass, M. Convolutional neural network and texture descriptor-based automatic detection and diagnosis of glaucoma. *Expert Systems with Applications*, 110, 250-263. (2018).
 29. Raghavendra, U., Bhandary, S. V., Gudigar, A., & Acharya, U. R. Novel expert system for glaucoma identification using non-parametric spatial envelope energy spectrum with fundus images. *Biocybernetics and Biomedical Engineering*, 38(1), 170-180. (2018).
 30. Maheshwari, S., Pachori, R. B., Kanhangad, V., Bhandary, S. V., & Acharya, U. R. Iterative variational mode decomposition based automated detection of glaucoma using fundus images. *Computers in biology and medicine*, 88, 142-149. (2017).
 31. Kausu, T. R., Gopi, V. P., Wahid, K. A., Doma, W., & Niwas, S. I. Combination of clinical and multiresolution features for glaucoma detection and its classification using fundus images. *Biocybernetics and Biomedical Engineering*, 38(2), 329-341. (2018).

32. Bowd, C., Belghith, A., Proudfoot, J. A., Zangwill, L. M., Christopher, M., Goldbaum, M. H., ... & Weinreb, R. N. (2020). Gradient Boosting Classifiers Combining Vessel Density and Tissue Thickness Measurements for Classifying Early to Moderate Glaucoma. *American Journal of Ophthalmology*
33. Santhi, D., Manimegalai, D., Parvathi, S., & Karkuzhali, S. (2016). Segmentation and classification of bright lesions to diagnose diabetic retinopathy in retinal images. *Biomedical Engineering/Biomedizinische Technik*, 61(4), 443-453.
34. Karkuzhali, S., & Manimegalai, D. (2017). Computational intelligence-based decision support system for glaucoma detection.
35. Santhi, D., Manimegalai, D., & Karkuzhali, S. (2014). Diagnosis of diabetic retinopathy by exudates detection using clustering techniques. *Biomedical Engineering: Applications, Basis and Communications*, 26(06), 1450077.
36. Karkuzhali, S., & Manimegalai, D. (2018). Retinal haemorrhages segmentation using improved toboggan segmentation algorithm in diabetic retinopathy images.
37. Karkuzhali, S., & Manimegalai, D. (2018). Detection of hemorrhages in retinal images using hybrid approach for diagnosis of diabetic retinopathy. *International Journal of Pure and Applied Mathematics*, 118(18), 2841-2846.
38. Karkuzhali, S., & Manimegalai, D. (2019). Robust intensity variation and inverse surface adaptive thresholding techniques for detection of optic disc and exudates in retinal fundus images. *Biocybernetics and Biomedical Engineering*, 39(3), 753-764.
39. Suriyasekeran, K., Santhanamahalingam, S., & Duraisamy, M. (2020). Algorithms for Diagnosis of Diabetic Retinopathy and Diabetic Macula Edema-A Review.
40. Karkuzhali, S., & Manimegalai, D. (2019). Distinguishing Proof of Diabetic Retinopathy Detection by Hybrid Approaches in Two Dimensional Retinal Fundus Images. *Journal of Medical Systems*, 43(6), 173.
41. Karkuzhali, S., & Manimegalai, D. (2018). Microaneurysms Identification using Computational Intelligence approach in Two Dimensional Fundus Images for detection of Diabetic Retinopathy. *International Journal of Pure and Applied Mathematics*, 118(8), 485-491.
42. Thakur, N., & Juneja, M. (2018). Survey on segmentation and classification approaches of optic cup and optic disc for diagnosis of glaucoma. *Biomedical Signal Processing and Control*, 42, 162-189.
43. Zilly, J., Buhmann, J. M., & Mahapatra, D. (2017). Glaucoma detection using entropy sampling and ensemble learning for automatic optic cup and disc segmentation. *Computerized Medical Imaging and Graphics*, 55, 28-41.
44. Divya, L., & Jacob, J. (2018). Performance analysis of Glaucoma detection approaches from fundus images. *Procedia computer science*, 143, 544-551
45. de Carvalho Junior, A. S. V., Carvalho, E. D., de Carvalho Filho, A. O., de Sousa, A. D., Silva, A. C., & Gattass, M. (2018). Automatic methods for diagnosis of glaucoma using texture descriptors based on phylogenetic diversity. *Computers & Electrical Engineering*, 71, 102-114.
46. Singh, A., Dutta, M. K., ParthaSarathi, M., Uher, V., & Burget, R. (2016). Image processing based automatic diagnosis of glaucoma using wavelet features of segmented optic disc from fundus image. *Computer methods and programs in biomedicine*, 124, 108-120.

47. Boquete, L., Miguel-Jiménez, J. M., Ortega, S., Rodríguez-Ascariz, J. M., Pérez-Rico, C., & Blanco, R. (2012). Multifocal electroretinogram diagnosis of glaucoma applying neural networks and structural pattern analysis. *Expert Systems with Applications*, 39(1), 234-238.
48. Acharya, U. R., Bhat, S., Koh, J. E., Bhandary, S. V., & Adeli, H. (2017). A novel algorithm to detect glaucoma risk using texton and local configuration pattern features extracted from fundus images. *Computers in biology and medicine*, 88, 72-83.
49. Mitra, A., Banerjee, P. S., Roy, S., Roy, S., & Setua, S. K. (2018). The region of interest localization for glaucoma analysis from retinal fundus image using deep learning. *Computer methods and programs in biomedicine*, 165, 25-35.
50. Issac, A., Sarathi, M. P., & Dutta, M. K. (2015). An adaptive threshold based image processing technique for improved glaucoma detection and classification. *Computer methods and programs in biomedicine*, 122(2), 229-244.
51. Miri M., S., Abràmoff, M. D., Kwon, Y. H., Sonka, M., & Garvin, M. K. (2017). A machine-learning graph-based approach for 3D segmentation of Bruch's membrane opening from glaucomatous SD-OCT volumes. *Medical image analysis*, 39, 206-217.
52. Medeiros, F. A., Jammal, A. A., & Thompson, A. C. (2019). From machine to machine: an OCT-trained deep learning algorithm for objective quantification of glaucomatous damage in fundus photographs. *Ophthalmology*, 126(4), 513-521.
53. Meriaudeau, F. (2018). Machine learning and deep learning approaches for retinal disease diagnosis. 3rd International Conference on Computer Science and Computational Intelligence 2018, *Procedia Computer Science* 135 (2018) 2
54. Mookiah, M. R. K., Acharya, U. R., Lim, C. M., Petznick, A., & Suri, J. S. (2012). Data mining technique for automated diagnosis of glaucoma using higher order spectra and wavelet energy features. *Knowledge-Based Systems*, 33, 73-82.
55. Niwas, S.I., Jakhetiya, V., Lin, W., Kwoh, C.K., Sng, C.C., Aquino, M.C., Victor, K. and Chew, P.T., 2016. Complex wavelet based quality assessment for AS-OCT images with application to Angle Closure Glaucoma diagnosis. *Computer methods and programs in biomedicine*, 130, pp.13-21.
56. Niwas, S.I., Lin, W., Bai, X., Kwoh, C.K., Kuo, C.C.J., Sng, C.C., Aquino, M.C. and Chew, P.T., 2016. Automated anterior segment OCT image analysis for Angle Closure Glaucoma mechanisms classification. *Computer methods and programs in biomedicine*, 130, pp.65-75.
57. Asaoka, R., Hirasawa, K., Iwase, A., Fujino, Y., Murata, H., Shoji, N., & Araie, M. (2017). Validating the usefulness of the "random forests" classifier to diagnose early glaucoma with optical coherence tomography. *American journal of ophthalmology*, 174, 95-103.
58. Cheng, L., Ding, Y., Hao, K., & Hu, Y. (2012). An ensemble kernel classifier with immune clonal selection algorithm for automatic discriminant of primary open-angle glaucoma. *Neurocomputing*, 83, 1-11.
59. Acharya, U. R., Ng, E. Y. K., Eugene, L. W. J., Noronha, K. P., Min, L. C., Nayak, K. P., & Bhandary, S. V. (2015). Decision support system for the glaucoma using Gabor transformation. *Biomedical Signal Processing and Control*, 15, 18-26.

60. Rehman, Z. U., Naqvi, S. S., Khan, T. M., Arsalan, M., Khan, M. A., & Khalil, M. A. (2019). Multi-parametric optic disc segmentation using superpixel based feature classification. *Expert Systems with Applications*, 120, 461-473.
61. Suryasa, I. W., Rodríguez-Gámez, M., & Koldoris, T. (2021). Health and treatment of diabetes mellitus. *International Journal of Health Sciences*, 5(1), i-v. <https://doi.org/10.53730/ijhs.v5n1.2864>
62. Gaibullaeva, N. N. (2021). The role of clinical examination early diagnosis of glaucoma. *International Journal of Health & Medical Sciences*, 4(3), 333-337. <https://doi.org/10.31295/ijhms.v4n3.1745>

Table 2: Comparison of Performance measures of Existing method and proposed method

S.NO	Title of the Paper	Year	Author details	Methodology	Database	Number of Images	Performance Measures
1	Machine learning models based on the dimensionality reduction of standard automated perimetry data for glaucoma diagnosis	2019	Lee, S. D., Lee, J. H., Choi, Y. G., You, H. C., Kang, J. H., & Jun, C. H	four classifiers—linear discriminant analysis, naïve Bayes classifier, support vector machines, and artificial neural networks—and four dimensionality reduction methods—Pearson correlation coefficient-based variable selection, Markov blanket variable selection, the minimum redundancy maximum relevance algorithm, and principal component analysis	Kyung Hee University Hospital at Gangdong from March 2007 to June 2015	375 healthy and 257 glaucomatous eyes	Area Under the receiver operating Characteristic curve (AUC) of 0.912.
2	Human versus Machine: Comparing a Deep Learning Algorithm to Human Gratings for Detecting Glaucoma on Fundus Photographs	2020	Jammal, A.A., Thompson, A.C., Mariottoni, E.B., Berchuck, S.I., Urata, C.N., Estrela, T., Wakil, S.M., Costa, V.P. and Medeiros, F.A.,	Machine to Machine deep learning (M2M DL)	Duke Glaucoma Repository (Duke Eye Center)	32,820 pairs of fundus photos and SD OCT scans from 2,312 eyes of 1,198 subjects	AUC = 0.801 (95% CI: 0.757, 0.845) versus 0.775 (95% CI: 0.728, 0.823), respectively; P = 0.222
3	Machine learning-based predictive modeling of surgical intervention in glaucoma using systemic data from electronic health records	2019	Baxter, S. L., Marks, C., Kuo, T. T., Ohno-Machado, L., & Weisbro, R. N.	multivariable logistic regression, random forests, and artificial neural networks	EHR data from patients with glaucoma from the University of California, San Diego (UCSD) Clinical Data Warehouse with clinical encounters during a 5-year period from September 2013 to September 2018	385	AUC of 0.67
4	Detection of longitudinal visual	2018	Yousefi, S., Kiwaki, T.,	machine-learning-based index for glaucoma	Moorfields Eye Hospital, London, UK.	2085 eyes of 1214 normal or	sensitivity of global MD, region-wise,

	field progression in glaucoma using machine learning		Zheng, Y., Sugiura, H., Asaoka, R., Murata, H., Lemij, H. and Yamanishi, K	progression detection that outperforms global, region-wise, and point-wise indices.		glaucoma subjects	point-wise, and machine learning analyses in detecting progression in the eyes of the longitudinal dataset using the optimum parameters for each method were 44%, 54%, 55%, 72%, respectively
5	Towards multi-center glaucoma OCT image screening with semi-supervised joint structure and function multi-task learning	2020	Wang, X., Chen, H., Ran, A.R., Luo, L., Chan, P.P., Tham , C.C., Chang, R.T., Manni , S.S., Cheung, C.Y. and Heng, P.A	CNN, structure analysis and surrogate-driven function regression	HK dataset, Stanford dataset	975,400 B-scans from 4,877 volumes 246,200 B-scans from 1,231 volumes	Area Under ROC Curve (AUC) of 0.977 on HK dataset and 0.933 on Stanford dataset
6	An hybrid feature space from texture information and transfer learning for glaucoma classification	2020	11. Claro, M., Veras, R., Santana, A., Araújo, F., Silva, R., Almeida, J., & Leite, D	GLCM, CNN, GLCM, CaffeNet, VGG-s, VGG-m, VGG-f, Gain ratio, Random Forest	RIM-ONE-1, RIM-ONE-2, RIM-ONE-3, DRISHTI, HRF, JSIEC, ACRIMA	873,802	Kappa index, and an accuracy of 93.35% for the development set and 92.78% for the performance set
7	Using soft computing techniques to diagnose Glaucoma disease	2019	Al-Akhras, M., Alawairdhi, M., & Habib, M.	Support Vector Machines and Genetically-Optimized Artificial Neural Networks, pronounced machine learning algorithms	Real time database (Collected from 3 Hospitals)	106	Support Vector Machines technique with 100% specificity and 87% accuracy. Artificial Neural Network classified the images with 98% accuracy
8	Generative adversarial network and texture features applied to automatic glaucoma detection	2020	Bisneto, T. R. V., de Carvalho Filho, A. O., & Magalhães, D. M. V	training of a conditional Generative Adversarial Network for segmentation of the optical discs into retinal images; pre-processing through	RIM-ONE and Drishti-GS	556	Accuracy-100%
				enhancement and hole fill-in techniques; extraction of texture attributes using the index of taxonomic diversity; and validation of the proposal through three classifiers			
9	Wearable sensors for gait pattern examination in glaucoma patients.	2016	Ma, Y., Amiri , N., & Ghasemzadeh , H	signal processing algorithms for feature estimation and leverage machine learning as well as statistical analysis approaches for gait pattern examination	UCLA Stein Eye Institute	19	Accuracy-80%
10	Offline computer-aided diagnosis for Glaucoma detection using fundus images targeted at mobile devices	2020	Martins, J., Cardoso, J. S., & Soares, F.	CNN	Origa , Drishti-GS, RIM-ONE r1, RIM-ONE r2, RIM-ONE r3, Challenge , RIGA [14]	749	0.91 and 0.75 of Intersection over Union (IoU) in the optic disc and optic cup segmentation, respectively. With regards to the classification, an accuracy of 0.87 with a sensitivity of 0.85 and an AUC of 0.93 were attained.
11	Refuge challenge: A unified framework for evaluating automated methods for glaucoma assessment from fundus photographs	2020	Orlando, J.I., Fu, H., Breda, J.B., van Kester , K., Bathula , D.R., Diaz-Pinto, A., Fang, R., Heng, P.A., Kim, J., Lee, J. and Lee, J.	Deep Learning	REFUGE	1200	
12	Glaucoma classification based on intra-class and extra-class discriminative correlation and consensus ensemble classifier	2020	Kishore, B., & Ananthamoorthi , N. P.	Support Vector Machine (SVM), Random Forest (RF) and K-Nearest Neighbor (KNN) for classification	High Resolution Fundus (HRF) and DRIVE		accuracy of 99.2%